Original article

A numerical model to evaluate formation properties through pressure-transient analysis with alternate polymer flooding

Jia Zhang[1], Shiqing Cheng[1]*, Changyu Zhu[1], Le Luo[1]

[1]*College of Petroleum Engineering, China University of Petroleum, Beijing 102249, P. R. China*

Abstract:
A numerical pressure transient analysis method of composite model with alternate polymer flooding is presented, which is demonstrated by field test data provided by China National Petroleum Corporation. Polymer concentration distribution and viscosity distribution are obtained on the basis of polymer rheological model, considering shear effect, convection, diffusion, inaccessible pore volume and permeability reduction of polymer. Pressure analysis mathematical model is established by considering wellbore storage effect and skin effect. Type curves are then developed from mathematical model which have seven sections and parameter sensitivity is analyzed, among which the transient sections of low-concentration and high-concentration hydrolyzed polyacrylamides (HPAM) solution, high-concentration HPAM solution and crude oil show obvious concave shape on pressure derivative curve due to different viscosities of three zones. Formation parameters and viscosity distribution of polymer solution can be calculated by type-curve matching. The polymer flooding field tests prove that the three-zone composite model can reasonably calculate formation parameters in onshore oilfield with alternate polymer flooding, which demonstrate the application potential of the analysis method.

1. Introduction

Over the past several years, many enhanced oil recovery (EOR) methods were researched in laboratories and oilfields to improve oil recovery (Jamaloei et al., 2010; Yu et al., 2010; Ren et al., 2011; Bera et al., 2013; Farajzadeh et al., 2013; Shiran and Skauge, 2013; Ren et al., 2014; Zhang et al., 2015). However, polymer flooding is most commonly applied in oilfields, especially hydrolyzed polyacrylamides (HPAM) polymer flooding because of its low cost and high efficiency (Wyatt et al., 2011). High sweep efficiency is significant advantage of polymer flooding (Lake, 1989). There comes problems with long-term high-concentration polymer flooding: The great injection pressure, blocking up in the porous medium, which lead to change of reservoir characteristics. In order to improve the efficiency of polymer flooding, alternate flooding of high-concentration and low-concentration polymer solutions has been widely applied in reservoirs. However, mechanism study and pressure analysis models about this technology are scare. On the other hand, pressure analysis methods applied in water flooding reservoirs have been widely

developed, however, study of which applied in onshore reservoirs with alternate polymer flooding is still in the primary stage. Liu (1994) analyzes transient pressure behavior in a polymer flooding composite reservoir by considering wellbore storage effect and skin effect. Song (1996, 1997) develops pressure analysis models of Newtonian and non-Newtonian fluid composite oilfields and power law non-Newtonian fluid composite oilfields. This paper will discuss the application of pressure analysis model with alternate flooding of high-concentration and low-concentration HPAM solutions in onshore oilfield on the basis of composite model and three-zone composite model of polymer flooding (Yu et al., 2014; Zhu et al., 2017). According to the injection process, high-concentration HPAM solution is injected at the beginning, after a period of time, low-concentration HPAM solution is injected. Surrounding the injection well, the first zone is low-concentration HPAM solution, the second zone is high-concentration HPAM solution, the third zone is oil (Fig. 1).

HPAM solution is non-Newtonian fluid widely used in polymer flooding, the viscosity of which is significant to establish pressure transient analysis model. Many researchers
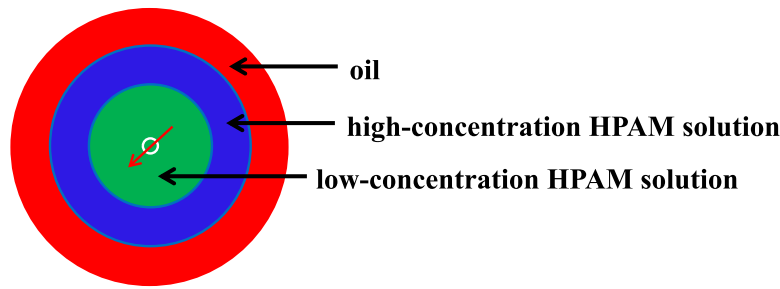
Fig. 1. Physical model of alternate flooding of high-concentration and low-concentration HPAM solutions.

Table 1. Characteristics of the proprietary HPAM polymer solution provided by CNPC.

μ_w (mPa·s)	A_1 (mg/L)$^{-1}$	A_2 (mg/L)$^{-2}$	A_3 (mg/L)$^{-3}$	D (cm^2/s)
0.5	6.34	1.93	9.21	0.0246

simply consider HPAM solution as power law fluid with constant power exponent model in polymer flooding oilfields (Zhang et al., 2010; Veerabhadrappa et al., 2013), which ignores interaction between polymer and reservoir rock, diffusion and convection of polymer. Meanwhile, the adsorption of polymer in formation porosity leads to inaccessible pore volume (IPV) (Liu et al., 2012) and permeability reduction, which also need to be taken into account. This paper establishes numerical method and analysis technology of three-zone composite model suitable for onshore oilfields with alternate polymer flooding, which taking wellbore storage effect, skin effect, convection, diffusion, inaccessible pore volume and permeability reduction into account. Moreover, field test data of alternate polymer flooding are further interpreted by this method.

2. Polymer rheological study

2.1 Rheological model

A proprietary HPAM used for polymer flooding is provided by China National Petroleum Corporation (CNPC). which is assumed as non-Newtonian fluid. As discussed above, the power law model (Bondor et al., 1972) or Carreau model (Carreau, 1968) both couldn't accurately explain rheological behavior of HPAM solution used in this paper. Polymer shear-thinning behavior is expressed by use of Meter equation (Eq. (1)) (Bourdet et al.,1989). The shear-thinning model applied in this paper match the apparent viscosity of proprietary HPAM solution very well provided by CNPC under extensive velocities.

$$\mu_p = \mu_\infty + \frac{\mu_p^0 - \mu_\infty}{1 + \left(\frac{\gamma}{\gamma_{1/2}}\right)^{Pa-1}} = \mu_w + \frac{\mu_p^0 - \mu_w}{1 + \left(\frac{\gamma}{\gamma_{1/2}}\right)^{Pa-1}} \quad (1)$$

where μ_p is viscosity of HPAM solution, mPa·s; μ_∞ is viscosity of HPAM solution at infinite shear rate, mPa·s, μ_w is water viscosity ; $\gamma_{1/2}$ is the shear rate when polymer viscosity is the mean of μ_∞ and μ_p^0, s^{-1}; γ is effective shear rate,

s^{-1}; Pa is fitting parameter; μ_p^0 is the viscosity when shear rate is very low (nearly zero), mPa·s, which is computed by modificatory Flory-Huggins equation (Flory, 1953):

$$\mu_p^0 = \mu_w \left[1 + \left(A_1 C_p + A_2 C_p{}^2 + A_3 C_p{}^3\right) C_{SEP}^{SP}\right] \quad (2)$$

where A_1, (mg/L)$^{-1}$, A_2, (mg/L)$^{-2}$, and A_3, (mg/L)$^{-3}$ are fitting parameters; C_p is polymer concentration, g/L; C_{SEP}^{SP} is coefficient expressing effect of salinity and hardness over polymer viscosity.

The HPAM solutions are disposed by mechanical stirring at 75 °C which is similar to oilfield temperature. The HPAM concentrations vary from 100 mg/L to 4000 mg/L. The polymer rheological measurement is conducted with Haake RS6000 rheometer. The HPAM viscosities of different concentrations are measured at 75 °C under 0.01 s^{-1} shear rate to get the fitting numbers of A_1, A_2, and A_3, which increase with increasing concentration of polymer solutions (Table 1).

Pa and $\gamma_{1/2}$ are functions of μ_p^0 (or polymer concentration). The expressions supplied by CNPC are shown in Eq. (3) and Eq. (4), respectively.

$$Pa = 1.163 \left(\mu_p^0\right)^{0.0311} \quad (3)$$

$$\gamma_{1/2} = 375.1 \left(\mu_p^0\right)^{-1.378} + 0.0356 \quad (4)$$

The expressions of effective shear rate and velocity are shown in Eq. (5) and Eq. (6) (Wang, 1990):

$$\gamma = \frac{3n+1}{n+1} \frac{10^4 v}{\sqrt{8C'K\phi}} \quad (5)$$

$$v = \frac{Q}{2\pi r h \phi} \quad (6)$$

where n is power law index of HPAM solution; C' is oilfield tortuosity coefficient; ϕ is oilfield porosity; K is oilfield permeability, μm^2; Q is injection rate of HPAM solution, m^3/s; h is oilfield thickness, m; r is radial distance from testing well, m; v is simplified Darcy velocity, m/s.

Considering inaccessible pore volume and permeability reduction caused by polymer flooding, Eq. (5) is changed to Eq. (7):

$$\gamma = \frac{3n+1}{n+1} \frac{10^4 v}{\sqrt{8C'K_p\phi_p}} \qquad (7)$$

where K_p is effective permeability, $K_p = K/R_k$, K is reservoir permeability; R_k is permeability reduction coefficient; ϕ_p is effective porosity, $\phi_p = \phi(1 - \text{IPV})$, ϕ is porosity, IPV is inaccessible pore volume fraction.

HPAM concentration equation considering effect of convection and diffusion is exhibited in Eq. (8) (Wang, 2008):

$$C_p(r,t) = \frac{C_{p0}}{2} - \frac{C_{p0}}{2} erf \left[\frac{r - vt}{2\sqrt{Dt}} \right] \qquad (8)$$

where C_{p0} is initial polymer concentration, g/L; D is diffusion coefficient of HPAM, cm^2/s; erf is error function; t is seepage time, s.

2.2 Polymer concentration distribution

When injection time (t_p) and injection rate (Q) of polymer solution are constant, polymer concentration ratio (C_p/C_{p0}) keeps high level in near-wellbore region, and drops dramatically with increasing radial distance (Fig. 2 and Fig. 3). Region of high-concentration ratio expands with increasing injection time (Fig. 2) or increasing injection rate (Fig. 3) of polymer solution.

2.3 Polymer viscosity distribution

According to the rheological model mentioned above, viscosity of polymer solution decreases with increasing effective shear rate, which is called polymer shear thinning, increases with increasing injection polymer concentration (Fig. 4). When injection polymer concentration, injection time and injection rate of polymer solution are constant, polymer solution viscosity increases firstly due to high shear rate in near-wellbore region and then decreases dramatically because of low-concentration in far-wellbore region. High viscosity region expands with increasing injection time or increasing injection rate due to accumulation of polymer, region of polymer shear thinning enlarges caused by increasing injection rate (Fig. 5 and Fig. 6).

3. Pressure analysis modeling methodology

Based on the rheological model and composite model discussed above (Zhu and Cheng, 2017), the pressure analysis interpretation model in composite reservoir with alternate polymer flooding is established, taking shear effect, diffusion, convection, inaccessible pore volume and permeability reduction of polymer, wellbore storage effect and skin effect into account. Mathematical model is written as Eq. (9) to Eq. (19).

The first zone:

$$\frac{1}{r} \frac{\partial}{\partial r} \left(r \frac{1}{\mu_{p1}} \frac{\partial p_1}{\partial r} \right) = \left(\frac{\phi_1 C_{t1}}{K_1} \right) \frac{\partial p_1}{\partial t} \quad (0 < r \leqslant r_{m1}) \qquad (9)$$
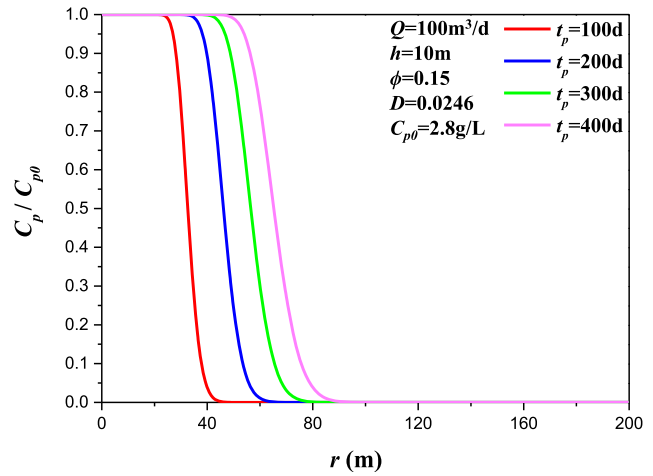
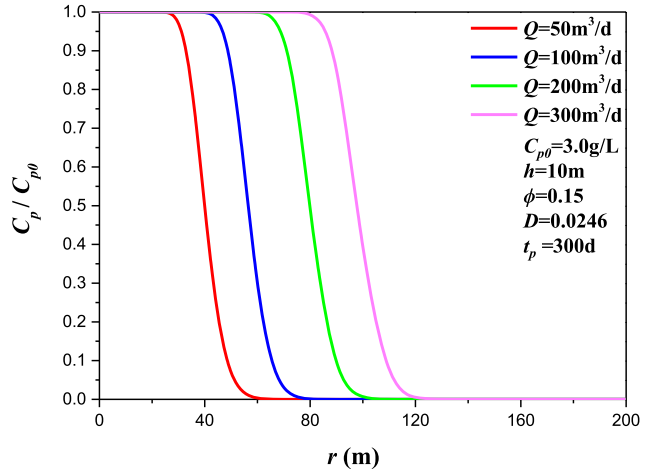**Fig. 2.** Effect of injection time of polymer solution on polymer concentration distribution.

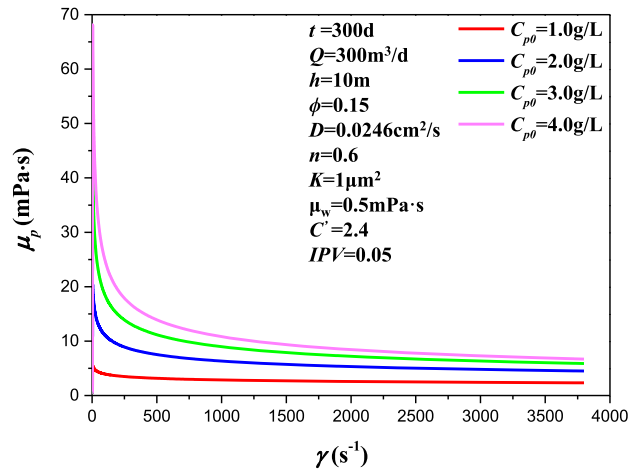**Fig. 3.** Effect of injection rate of polymer solution on polymer concentration distribution.

Fig. 4. Effect of injection concentration and effective shear rate of polymer solution on polymer viscosity.
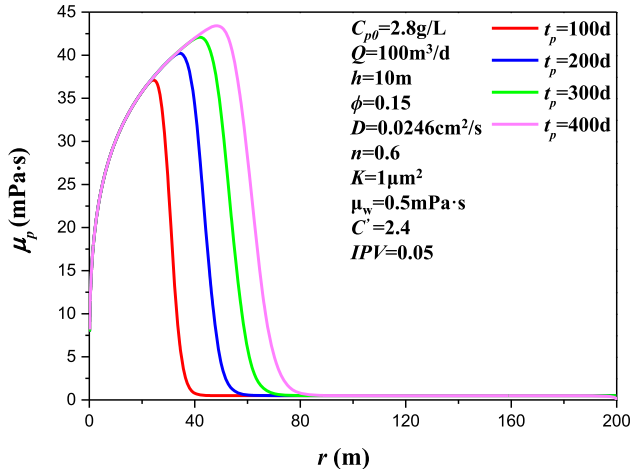
Fig. 5. Effect of injection time of polymer solution on polymer viscosity distribution.
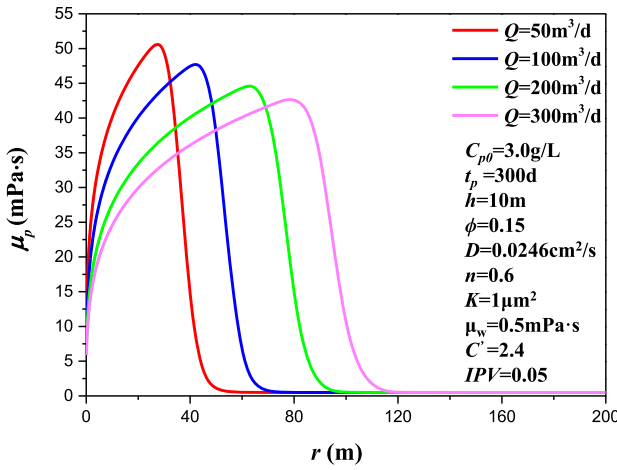

Fig. 6. Effect of injection rate of polymer solution on polymer viscosity distribution.

The second zone:

$$\frac{1}{r}\frac{\partial}{\partial r}\left(r\frac{1}{\mu_{p2}}\frac{\partial p_2}{\partial r}\right) = \left(\frac{\phi_2 C_{t2}}{K_2}\right)\frac{\partial p_2}{\partial t} \quad (r_{m1} < r \leqslant r_{m2}) \tag{10}$$

The third zone:

$$\frac{1}{r}\frac{\partial}{\partial r}\left(r\frac{\partial p_3}{\partial r}\right) = \mu_0\left(\frac{\phi_3 C_{t3}}{K_3}\right)\frac{\partial p_3}{\partial t} \quad (r > r_{m2}) \tag{11}$$

Internal boundary conditions:

$$QB = C\frac{dp_{wf}}{dt} - \left(\frac{2\pi r K_1 h}{\mu_{p1}}\frac{\partial P_1}{\partial r}\right)_{r=r_w} \tag{12}$$

$$p_{wf} - p\mid_{r=r_w} = -S\left(r\frac{\partial p_1}{\partial r}\right)_{r=r_w} \tag{13}$$

External boundary condition (infinite boundary):

$$p_3\left(r \to \infty, t\right) = p_i \tag{14}$$

At interface:

$$p_1\left(r = r_{m1}, t\right) = p_2 \quad (r = r_{m1}, t) \tag{15}$$

$$p_2\left(r = r_{m2}, t\right) = p_3 \quad (r = r_{m2}, t) \tag{16}$$

$$\frac{K_1}{\mu_{p1}}\frac{\partial p_1}{\partial r}\left(r = r_{m1}, t\right) = \frac{K_2}{\mu_{p2}}\frac{\partial p_2}{\partial r} \quad (r = r_{m1}, t) \tag{17}$$

$$\frac{K_2}{\mu_{p2}}\frac{\partial p_2}{\partial r}\left(r = r_{m2}, t\right) = \frac{K_3}{\mu_o}\frac{\partial p_3}{\partial r} \quad (r = r_{m2}, t) \tag{18}$$

Initial condition:

$$p_1\left(r, t = 0\right) = p_2\left(r, t = 0\right) = p_3\left(r, t = 0\right) = p_i \tag{19}$$

where p_1, ϕ_1, C_{t1}, K_1 is respectively pressure (MPa), porosity, total compressibility (MPa^{-1}), permeability (μm^2) of the first zone; p_2, ϕ_2, C_{t2}, K_2 is respectively pressure (MPa), porosity, total compressibility (MPa^{-1}), permeability (μm^2) of the second zone; p_3, ϕ_3, C_{t3}, K_3 is respectively pressure (MPa), porosity, total compressibility (MPa^{-1}), permeability (μm^2) of the third zone; p_i is primitive oilfield pressure, MPa; p_{wf} is bottom hole pressure, MPa; C is wellbore storage coefficient, m^3/MPa; B is volume factor of polymer solution; S is skin factor; R_{m1} is radius of the first zone, m; R_{m2} is radius of the second zone, m; μ_{p1} is viscosity of low-concentration polymer solution in the first zone, mPa·s; μ_{p2} is viscosity of high-concentration polymer solution in the second zone, mPa·s; μ_o is oil viscosity in the third zone, mPa·s.

Dimensionless parameters are developed to analyze bottom-hole pressure excluding the effect of some oilfield parameters, which is written as Eq. (20) to Eq. (25):

$$p_D = \frac{Kh}{1.842 \times 10^{-3} Q\mu_{p1}B}\left(p - p_i\right) \tag{20}$$

$$p_{wD} = \frac{Kh}{1.842 \times 10^{-3} Q\mu_{p1}B}\left(p_w - p_i\right) \tag{21}$$

$$t_D = \frac{3.6K}{\phi\mu_{p1}C_t r_w^2}t \tag{22}$$

$$C_D = \frac{C}{2\pi h\phi C_t r_w^2} \tag{23}$$

$$r_D = \frac{r}{r_w} \tag{24}$$

$$p'_{wD} = \frac{\Delta p_{wD}}{\Delta t_D} \tag{25}$$

where p_D is dimensionless pressure; p_{wD} is dimensionless bottom-hole pressure; p'_{wD} is derivative of dimensionless bottom-hole pressure; t_D is dimensionless time; Δp_{wD} is difference of dimensionless bottom-hole pressure; Δt_D is difference of dimensionless time difference; C_D is dimensionless wellbore storage coefficient; r_D is dimensionless distance; r_w is wellbore radius, m.

4. Results and discussion

4.1 Formation pressure difference

The formation pressure grows with increasing injection time of polymer solution during alternate polymer flooding. On the basis of dimensionless pressure difference and dimensionless distance, the curves of pressure difference at different time are obtained. When the radius of first zone is 110 m and the radius of second zone is 298 m, pressure difference grows with increasing injection time of low-concentration polymer solution and decreases with increasing distance (Fig. 7).

4.2 Type curves and sensitivity analysis

On the basis of dimensionless bottom-hole pressure (BHP) and derivative of dimensionless BHP, type curves in log-log scale are obtained, which have seven flow sections (Fig. 8): (I) wellbore storage section; (II) intermediate flow section (transient section), that describes pressure response between wellbore storage stage and first radial flow stage; (III) first radial flow section; (IV) transient section of low-concentration and high-concentration polymer solution, pressure derivative curve of which exhibiting an evident upturn; (V) second radial flow section, pressure derivative curve of which showing a slope due to high-concentration of the HPAM solution; (VI) transient section of high-concentration HPAM solution and oil; (VII) combination section (effected by three zones at the same time).

The effects of various parameters on type curves are analyzed, including injection concentration of polymer solution, radius of first zone, radius of second zone and permeability of every zone.

4.2.1 Injection concentration of HPAM solution

The effect of injection concentration of low-concentration HPAM solution on type curves in composite reservoir with alternate polymer flooding is exhibited in Fig. 9. The higher injection concentration of low-concentration HPAM solution is, the larger flow resistance is in first zone, that leading to pressure derivative curve moving up in transient flow section (II) and first radial flow section (III), while other sections are not influenced.

The effect of injection concentration of high-concentration HPAM solution on type curves in composite reservoir with alternate polymer flooding is shown in Fig. 10. The increasing injection concentration of high-concentration HPAM solution leads to pressure derivative curve moving up in transient section (IV), second radial flow section (V), transient section of high-concentration HPAM solution and oil (VI).

4.2.2 Composite radius

The effect of first zone radius on type curves in composite reservoir with alternate HPAM solution flooding is exhibited in Fig. 11. The first zone radius manifests injection time of low-concentration HPAM solution and sweeping volume of low-concentration HPAM solution. When second radius keeps
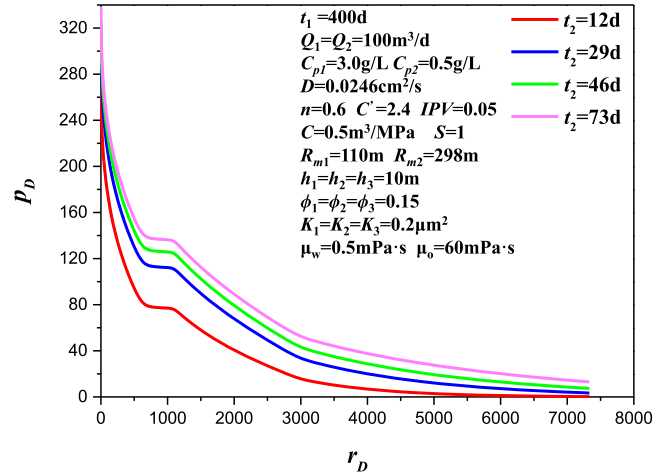

Fig. 7. Effect of injection time of low-concentration polymer solution on pressure difference distribution.
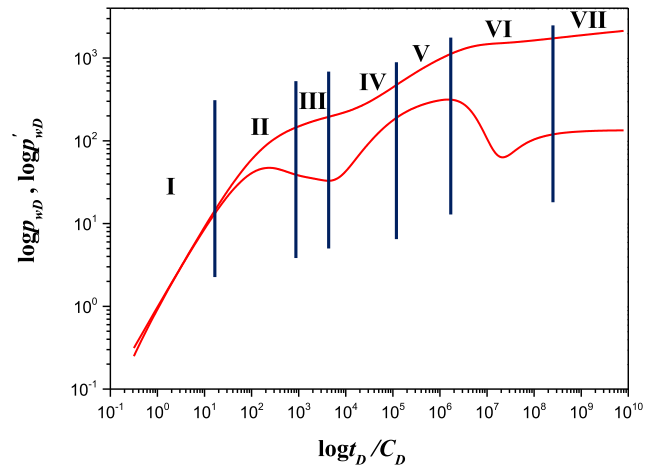

Fig. 8. Type curves of pressure transient analysis in three-zone composite reservoir with alternate HPAM flooding.
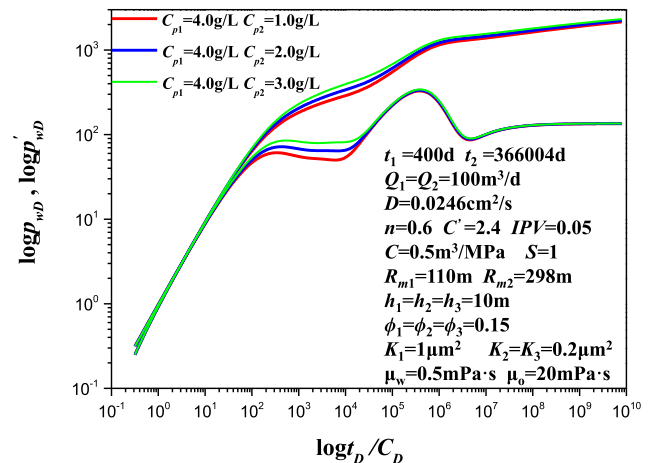

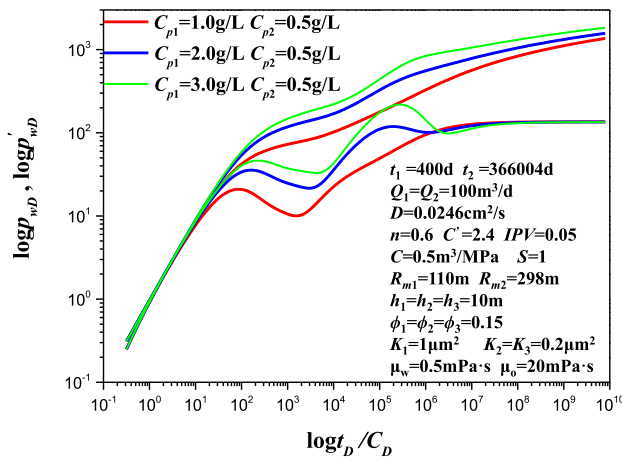**Fig. 9.** Effect of injection concentration of low-concentration HPAM solution on type curves.

Fig. 10. Effect of injection concentration of high-concentration HPAM solution on type curves.
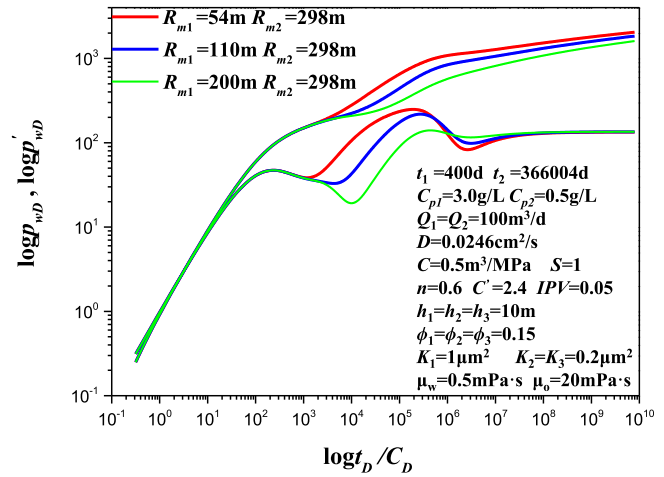

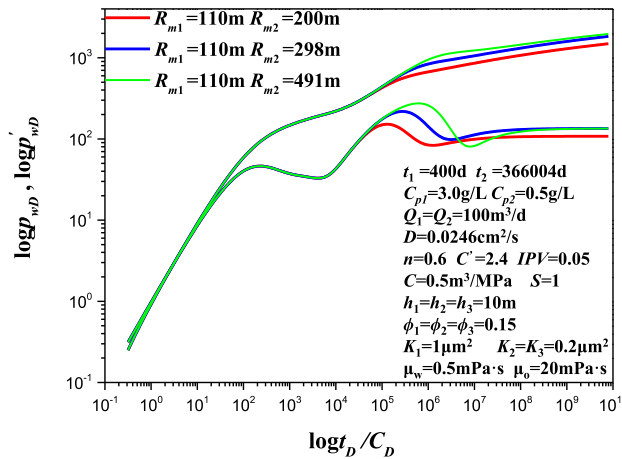**Fig. 11.** Effect of the first zone radius on type curves.

Fig. 12. Effect of the second zone radius on type curves.
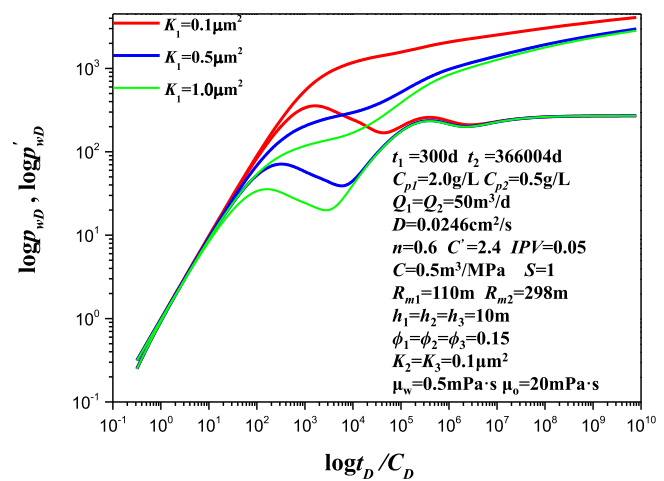

Fig. 13. Effect of first zone permeability on type curves.

invariable, the larger first zone radius is, the longer injection time of first radial flow section (III) is, which resulting in transient section (IV) appearing later. Nevertheless, pressure derivative curves will overlap at last in combination section (VII), because first zone radius do not influence mobility of other regions.

The effect of second zone radius on type curves in composite reservoir with HPAM flooding is exhibited in Fig. 12. The second zone radius manifests injection time of high-concentration HPAM solution and sweeping volume of high-concentration HPAM solution. When first radius keeps invariable, the larger second zone radius is, the longer injection time of second radial flow section (V) is, which causing transient section (VI) emerging later. But pressure derivative curves overlap in first radial flow section (III), intermediate section (IV) and combination section (VII).

4.2.3 Permeability

The effect of first zone permeability on typical curves in composite reservoir with HPAM flooding is exhibited in Fig.

13. Pressure curve and pressure derivative curve move downward and emerge early in transient section (II), first radial flow section (III) and transient section (IV) with increasing first zone permeability, which causing pressure loss decreasing. However, pressure derivative curves of other sections keep overlapping, which are not influenced by first zone permeability.

Pressure derivative curve move downward in transient section (IV), second radial flow section (V) and transient section (VI) with increasing second zone permeability, while pressure derivative curves of other sections are convergent (Fig. 14).

Pressure curve and pressure derivative curve move downward in transient section (VI) and combination section (VII) with increasing third zone permeability, while pressure derivative curves of other sections are convergent (Fig. 15).

5. Field tests interpretation

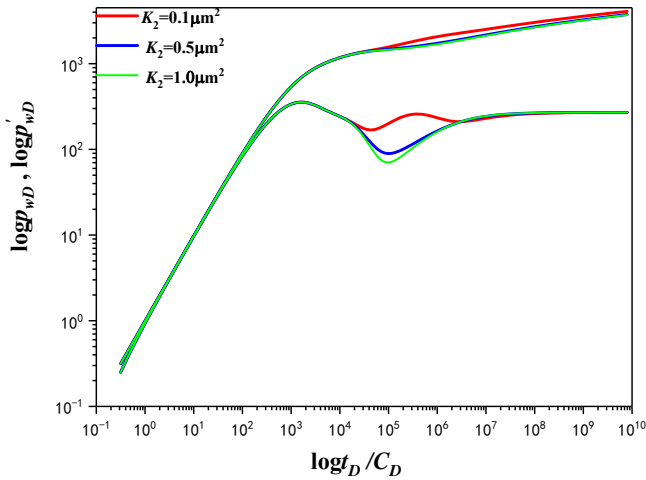Pressure analysis data of field test was provided by CNPC.

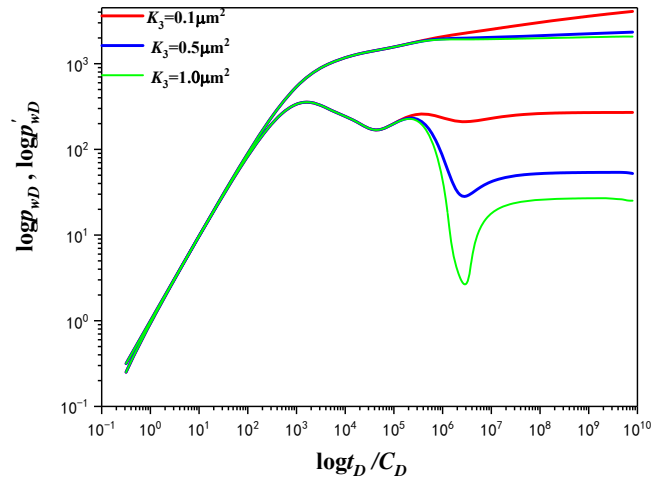**Fig. 14.** Effect of second zone permeability on type curves.

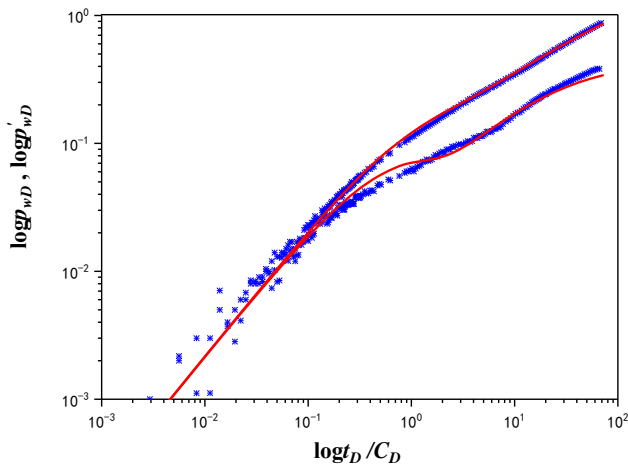**Fig. 15.** Effect of third zone permeability on type curves.

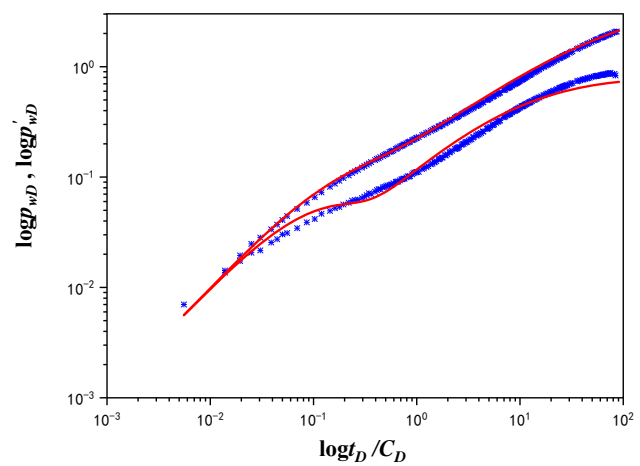**Fig. 16.** Well 1 field test data and matching curves.

Fig. 17. Well 2 field test data and matching curves.

First draw pressure curve and pressure derivative curve of field test data with time in log-log scale and modify smoothing of curves with Bourdet's method (Yu et al., 2014). Then draw pressure curve and pressure derivative curve with basic oilfield parameters and assuming interpreting parameters using models studied above. Finally, adjust assuming interpreting parameters and perform history matching to get right outcome of three-zone composite oilfield with alternate HPAM solution flooding until curves deriving from model and field test data overlapping. In this way, average formation pressure, permeability of every zone, composite radius, skin factor, wellbore storage coefficient and so on would be calculated, which is basis of adjusting development plan.

Well 1 performed HPAM flooding with injection concentration of 1200 mg/L from Sep. 1, 2014 to Aug. 2, 2015, with injection concentration of 600 mg/L from Aug. 3, 2015 to Oct. 9, 2015, then polymer injection was stopped and pressures were measured for three days. Well 2 performed HPAM flooding with injection concentration of 1600 mg/L

from Sep. 2, 2015 to Mar. 9, 2017, with injection concentration of 600 mg/L from Mar. 10, 2017 to Jun. 7, 2017, then polymer injection was ceased and pressures were measured for four days. Basic data of well 1 and well 2 are exhibited in Table 2. Field testing data and matching curves are exhibited in Fig. 16 and Fig. 17, interpretation outcomes are exhibited in Table 3. The permeability by interpreting field test data conform to practical oilfield, demonstrating that model presented in this paper could analyze field pressure test and assess formation.

6. Conclusion

This work establishes pressure analysis models for three-zone composite reservoirs with alternate HPAM flooding. Type curves and sensitivity analysis are accomplished on the basis of numerical solution, at last interpreting parameters are acquired by matching of field test data and type curves. Three conclusions are summarized from the study above.

(1) Polymer concentration distribution, viscosity distribu-

Table 2. Basic parameters of wells and reservoir for field tests.

Parameters	Units	Well 1	Well 2
Injection rate	Q (m^3/d)	34	19
Porosity	ϕ	0.158	0.158
Crude oil viscosity	μ_o (mPa·s)	5.84	5.84
Total compressibility	C_t (MPa^{-1})	0.002	0.002
Well radius	r_w (m)	0.07	0.07
Volume factor	B_o	1.175	1.175
Formation thickness	h	18.5	12.5
Permeability before polymer flooding	K (μm^2)	0.25	0.25

Table 3. Interpretation results of well 1 and well 2.

Parameters	Units	Well 1	Well 2
Average reservoir pressure	p_i (MPa)	22.41	22.74
The first zone permeability	K_1 (μm^2)	0.151	0.153
The second zone permeability	K_2 (μm^2)	0.025	0.011
The third zone permeability	K_3 (μm^2)	0.021	0.009
The first radius	R_{m1} (m)	45.3	20.2
The second radius	R_{m2} (m)	150.5	241.6
Skin factor	S	1	1
Wellbore storage coefficient	C (m^3/MPa)	6.49	0.74

tion, and the pressure analysis model developed in this work by considering IPV, permeability reduction, shear rate, diffusion, and convection accord with rheological characteristic of HPAM solution provided by CNPC.

(2) Sensitivity analysis is performed to study the effect of different parameters on type curves, incorporating injection polymer concentration, composite radius and permeability of every zone.

(3) Field tests are conducted in two wells of three-zone composite reservoirs with alternate HPAM flooding. The model presented in this paper is applied to match field test data to obtain interpreting parameters of oilfield, which demonstrates the accuracy of pressure transient analysis method.

Nomenclature

μ_p = viscosity of HPAM solution, mPa·s
μ_∞ = viscosity of HPAM solution at infinite shear rate, mPa·s
μ_w = brine viscosity, mPa·s
μ_p^0 = viscosity when shear rate is very low (nearly zero), mPa·s
$\gamma_{1/2}$ = the shear rate when viscosity is mean of μ_∞ and μ_p^0, s^{-1}
γ = effective shear rate, s^{-1}
Pa = fitting parameter
A_1 = fitting parameter, (mg/L)$^{-1}$
A_2 = fitting parameter, (mg/L)$^{-2}$
A_3 = fitting parameter, (mg/L)$^{-3}$

C_p = polymer concentration, g/L
C_{SEP}^{SP} = coefficient expresses effect of salinity and hardness over polymer viscosity
n = power law index of HPAM solution
C' = oilfield tortuosity coefficient
ϕ = oilfield porosity
K = oilfield permeability, μm^2
Q = injection rate of HPAM solution, m^3/s
$Q1$ = injection rate of high-concentration polymer solution, m^3/d
$Q2$ = injection rate of low-concentration polymer solution, m^3/d
h = reservoir thickness, m
r = radial distance, m
v = Darcy velocity, m/s
R_k = permeability reduction coefficient
K_p = effective permeability, μm^2
IPV = inaccessible pore volume fraction
ϕ_p = effective porosity
C_{p0} = injection concentration of HPAM solution, g/L
D = diffusion coefficient of HPAM, cm^2/s
erf = error function
t = seepage time, s
t_1 = injection time of high-concentration polymer solution, d
t_2 = injection time of low-concentration polymer solution, d
p_1 = pressure of the first zone, MPa
ϕ_1 = porosity of the first zone

C_{t1} = total compressibility of the first zone, MPa^{-1}
K_1 = permeability of the first zone, μm^2
p_2 = pressure of the second zone, MPa
ϕ_2 = porosity of the second zone
C_{t2} = total compressibility of the second zone, MPa^{-1}
K_2 = permeability of the second zone, μm^2
p_3 = pressure of the third zone, MPa
ϕ_3 = porosity of the third zone
C_{t3} = total compressibility of the third zone, MPa^{-1}
K_3 = permeability of the third zone, μm^2
p_i = primitive oilfield pressure, MPa
p_{wf} = bottom hole pressure, MPa
C = wellbore storage coefficient, m^3/MPa
B = volume factor of polymer solution
B_o = volume factor of oil
S = skin factor
R_{m1} = radius of the first zone, m
R_{m2} = radius of the second zone, m
μ_{p1} = viscosity of low-concentration polymer solution in the first zone, mPa·s
μ_{p2} = viscosity of high-concentration polymer solution in the second zone, mPa·s
μ_o = crude oil viscosity in the third zone, mPa·s
p_D = dimensionless pressure
p_{wD} = dimensionless bottom hole pressure
t_D = dimensionless time
C_D = dimensionless wellbore storage coefficient
r_D = dimensionless distance
r_w = wellbore radius, m
p'_{wD} = derivative of dimensionless bottom hole pressure
Δp_{wD} = difference of dimensionless bottom hole pressure
Δt_D = difference of dimensionless time
BHP = bottom hole pressure
CNPC = China National Petroleum Corporation

Acknowledgments

References

Bera, A., Mandal, A., Guha, B.B. Synergistic effect of surfactant and salt mixture on interfacial tension reduction between crude oil and water in enhanced oil recovery. J. Chem. Eng. Data 2013, 59(1): 89-96.

Bondor, P.L., Hirasaki, G.J., Tham, M.J. Mathematical simulation of polymer flooding in complex reservoirs. SPE J. 1972, 12(5): 369-382.

Bourdet, D., Ayoub, J.A., Pirard, Y.M. Use of pressure derivative in well test interpretation. SPE Form. Eval. 1989, 4(2): 293-302.

Carreau, P.J. Rheological equations from molecular network theories. Madison, USA, University of Wisconsin-Madison, 1968.

Farajzadeh, R., Ameri, A., Faber, M.J., et al. Effect of continuous, trapped, and flowing gas on performance of alkaline surfactant polymer (ASP) flooding. Ind. Eng. Chem. Res. 2013, 52(38): 13839-13848.

Flory, P.J. Principles of Polymer Chemistry. New York, USA, Cornell University Press, 1953.

Jamaloei, B.Y., Kharrat, R., Torabi, F. Analysis and correlations of viscous fingering in low-tension polymer flooding in heavy oil reservoirs. Energ. Fuel. 2010, 24(12): 6384-6392.

Lake, L.W. Enhanced Oil Recovery. Boston, USA, Prentice Hall, 1996.

Liu, J., Guo, Y., Hu, J., et al. Displacement characters of combination flooding systems consisting of gemini-nonionic mixed surfactant and hydrophobically associating polyacrylamide for Bohai offshore oilfield. Energ. Fuel. 2012, 26(5): 2858-2864.

Liu, Y., Yan, B., Zhai, Y., et al. Transient pressure behavior in a homogeneous composite reservoir. Acta. Petrol. Sin. 1994, 15(1): 92-100.

Meter, D.M., Bird, R.B. Tube flow of non-Newtonian polymer solutions: PART I. Laminar flow and rheological models. AIChE J. 1964, 10(6): 878-881.

Ren, G., Sanders, A.W., Nguyen, Q.P. New method for the determination of surfactant solubility and partitioning between CO_2 and brine. J. Supercrit. Fluid. 2014, 91: 77-83.

Ren, G., Zhang, H., Nguyen, Q.P. Effect of surfactant partitioning between CO_2 and water on CO_2 mobility control in hydrocarbon reservoirs. Paper SPE145102 Presented at the SPE Enhanced Oil Recovery Conference, Kuala Lumpur, Malaysia, 19-21 July, 2011.

Shiran, B.S., Skauge, A. Enhanced oil recovery (EOR) by combined low salinity water/polymer flooding. Energ. Fuel. 2013, 27(3): 1223-1235.

Song, K. Well test analysis of a compound reservoir with non-Newtonian and Newtonian fluid flow. Acta. Petrol. Sin. 1996, 17: 82-86.

Song, K., Zhu, J. Well test analysis for a compound reservoir with non-Newtonian power-law fluids flow. Acta. Petrol. Sin. 1997, 18: 78-83.

Veerabhadrappa, S.K., Trivedi, J.J., Kuru, E. Visual confirmation of the elasticity dependence of unstable secondary polymer floods. Ind. Eng. Chem. Res. 2013, 52(18): 6234-6241.

Wang, J. Physic-Chemical Fluid Mechanics and Application in Chemical EOR. Beijing, China, Petroleum Industry Press, 2008.

Wang, X. Determination of the main parameters in the numerical simulation of polymer flooding. Petrol. Explor. Dev. 1990, 3: 69-76.

Wyatt, N.B., Gunther, C.M., Liberatore, M.W. Increasing viscosity in entangled polyelectrolyte solutions by the addition of salt. Polymer 2011, 52(11): 2437-2444.

Yu, H., Guo, H., Cheng, S., et al. Numerical well testing interpretation method of composite model and applications in offshore reservoirs by polymer flooding. Asian J. Chem. 2014, 26(17): 5783-5788.

Yu, H., Kotsmar, C., Yoon, K.Y., et al. Transport and retention of aqueous dispersions of paramagnetic nanoparticles in reservoir rocks. Paper SPE129887 Presented at the SPE Improved Oil Recovery Symposium, Tulsa, Oklahoma, USA, 24-28 April, 2010.

Zhang, H., Challa, R.S., Bai, B., et al. Using screening test results to predict the effective viscosity of swollen superabsorbent polymer particles extrusion through an open fracture. Ind. Eng. Chem. Res. 2010, 49(23): 12284-12293.

Zhang, T., Murphy, M.J., Yu, H., et al. Investigation of nanoparticle adsorption during transport in porous media. SPE J. 2015, 20(4): 667-677.

Zhu, C., Cheng, S., He, Y., et al. Pressure transient behavior for alternating polymer flooding in a three-zone composite reservoir. Polym. Polym. Compos. 2017, 25(1): 1-10.